# Supplementary Information

# Synthesis and $CO_2$ photoreduction of two 3d–4f heterometal–organic frameworks

Yu Yang,[a] Yaomei Fu,[b] Siqi You,[a] Mingyue Li,[a] Chao Qin,[*a] Liang Zhao[*a] and Zhongmin Su[a]

[a]Key Laboratory of Polyoxometalate and Reticular Material Chemistry of Ministry of Education, Northeast Normal University. Changchun, Jilin, 130024 (China).
Email: qinc703@nenu.edu.cn; zhaol352@nenu.edu.cn

[b]Shandong Peninsula Engineering Research Center of Comprehensive Brine Utilization, Weifang University of Science and Technology, Shouguang, 262700 (China)

## Experimental Procedures

### Materials

All the reagents were purchased from chemical suppliers without any further purification.

### Characterization

The elemental analyses of C, H, and N were performed on a Perkin-Elmer 2400 CHN elemental analyzer. X-ray diffraction patterns (PXRD) were recorded on a Siemens D5005 diffractometer with graphite-monochromatized Cu Kα (λ = 1.5418 Å) radiation. The Fourier transform infrared (FT-IR) spectra were recorded in the range of 4000–400 $cm^{-1}$ using a Matton Alpha-Centauri FT-IR spectrophotometer with KBr pellets. Thermogravimetric analyses (TGA) were performed using a Perkin-Elmer TG-7 analyzer heated from 25 °C to 800 °C under $N_2$ at a heating rate of 10 °C $min^{-1}$. The UV–vis absorption spectra were recorded on a Shimadzu UV-2550 spectrophotometer in the range of 200–1600 nm. Steady-state photoluminescence (PL) spectra and time-resolved PL decay spectra were performed on a Spectrometer (Hitachi F-4600). The photoluminescent quenching of $[Ru(bpy)_3]Cl_2$ (7 mg) were performed in the 4mL MeCN of increasing amounts of catalyst (0, 0.25, 0.5, 0.75, and 1.0 mg) respectively.

### Single-Crystal X-ray Crystallography

Single-crystal diffraction data were recorded on a Bruker Apex CCD II diffractometer at 296 K, with graphitemonochromated Mo-K$\alpha$ radiation ($\lambda$ = 0.71073 Å). The data frames were recorded and processed using the APEX 2 suite of programs. The data were corrected for absorption and beam corrections based on the multi-scan technique as implemented in SADABS. The structures were solved by the direct method using SHELXS or SHELXT and refined by fullmatrix least-squares on $F^2$ using the SHELXL software.

**Electrochemical Measurements**

The Mott-Schottky plots were measured on an electrochemical system (CHI760e) via a conventional three-electrode system in a 0.1 M acetonitrile solution of tetrabutylammonium hexafluorophosphate. The 6mg catalyst was dispersed in 1 mL acetonitrile solution to produce homogeneous slurry. Subsequently, 60 µL of the slurry was transferred to a fluoride-tin oxide (FTO) glass plate covered with about 1 $cm^2$ of platinum plate as a counter at frequencies of 500, 800 and 1000 Hz, Ag / AgCl were used as reference electrodes.

## Results and Discussion

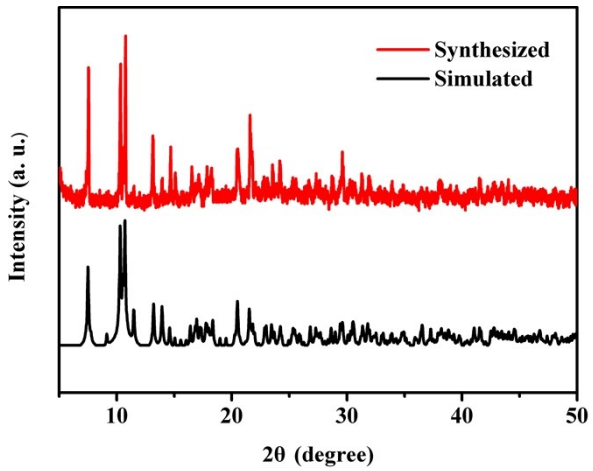


**Fig. S1** PXRD patterns of **1** with simulated (black line), as-synthesized (red line).

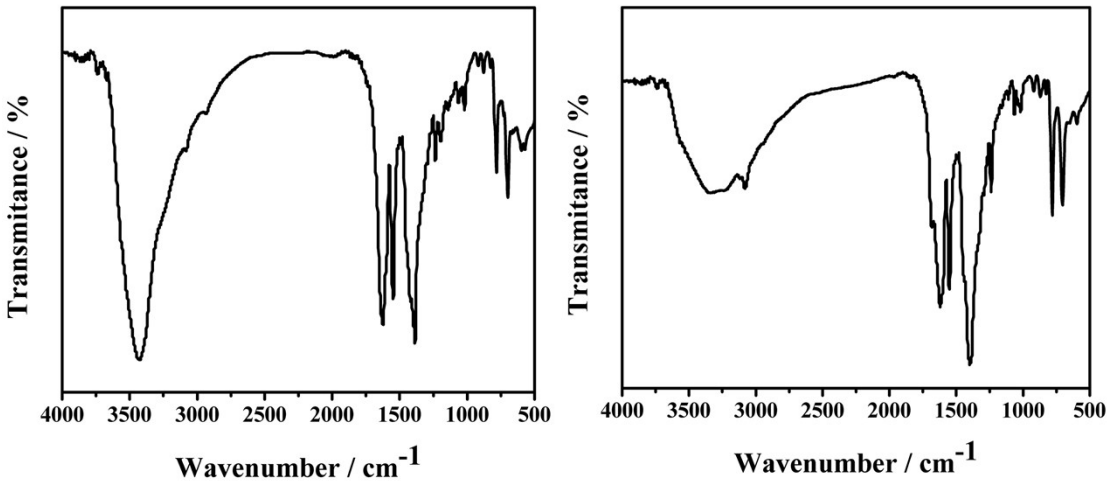


**Fig. S2** IR spectra of **1** (left) and **2**(right).

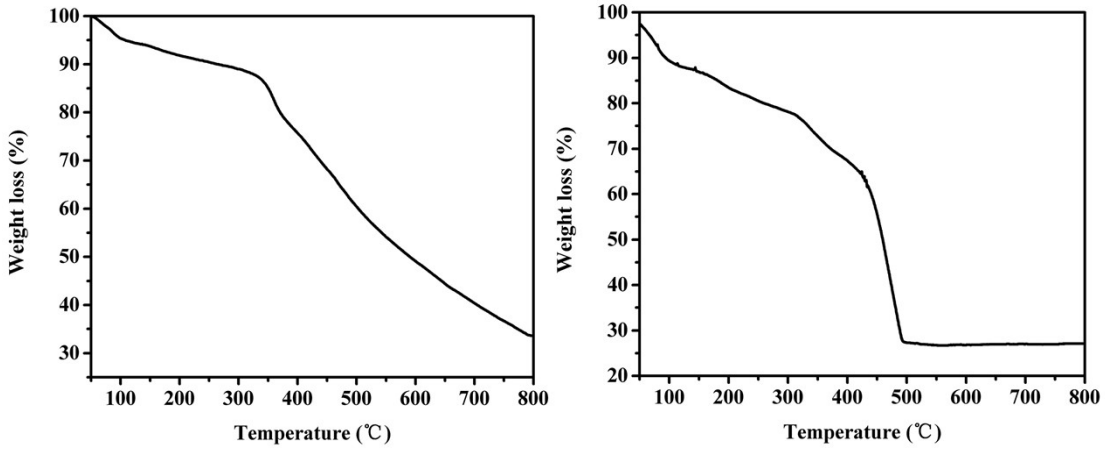


**Fig. S3** TG curves of **1** (left) and **2** (right).

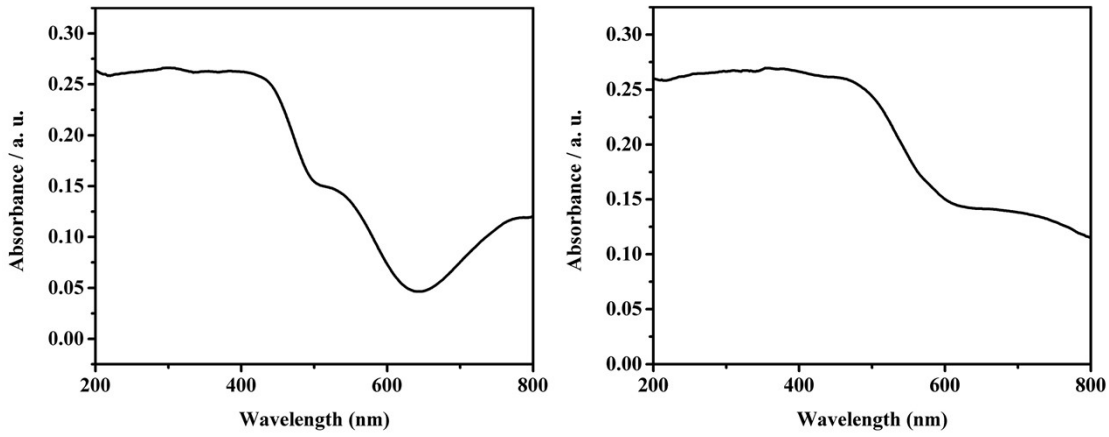


**Fig. S4** UV-Vis spectra of **1** (left) and **2**(right).

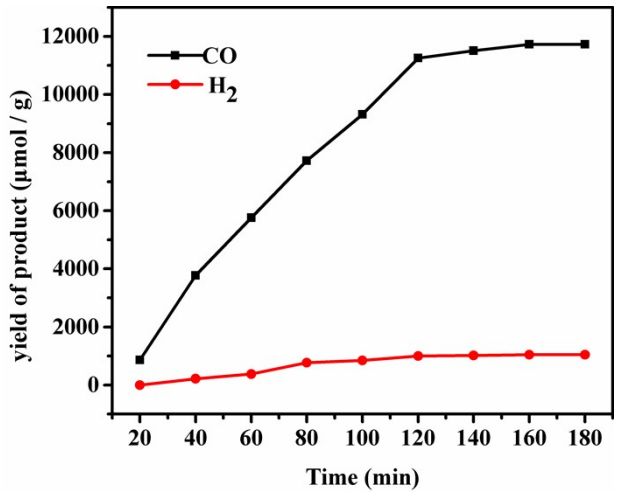


**Fig. S5** Product of CO and $H_2$ evolution catalyzed by **2** in the presence of $CO_2$–saturated $CH_3CN/TEOA/H_2O$ (4:1:1, V:V:V) solvent mixture under irradiation using a 300 W Xe lamp at 293K.

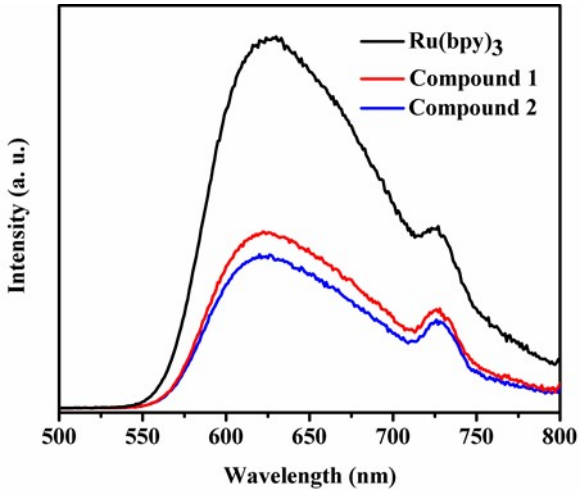


**Fig. S6** Effect of adding 1mg **1** and **2** on the steady−state fluorescence spectra of $[Ru(bpy)_3]Cl_2$.

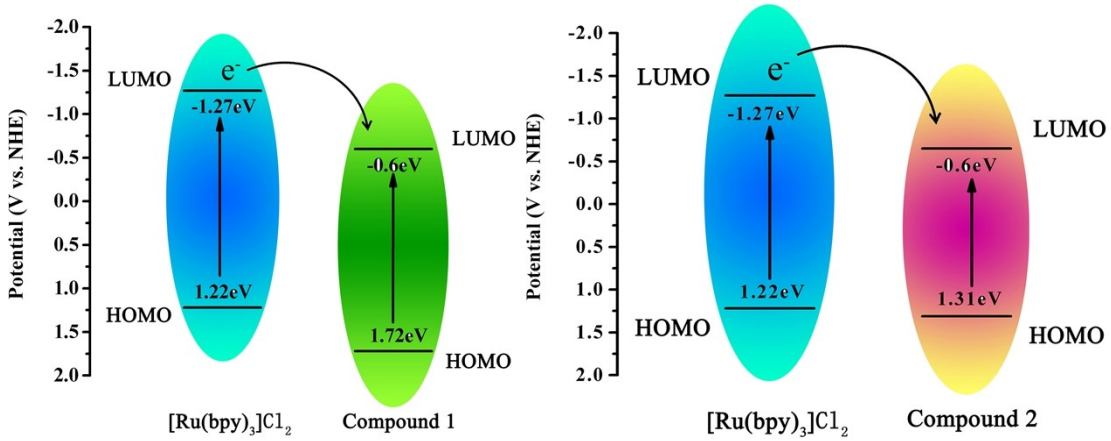


**Fig. S7** The schematic energy-level diagrams showing electron transfer form $[Ru(bpy)_3]^{2+}$ to **1** (left) and **2** (right).

**Table S1. Crystal data and structure refinements for 1 and 2**

| Compound | **1** | **2** |
|---|---|---|
| Empirical formula | $C_{40}H_{33}Gd_2N_9NiO_{23}$ | $C_{44}H_{48}CoGd_2N_9O_{23}$ |
| Formula weight | 1380.96 | 1444.34 |
| Temperature/K | 173.02 | 173.02 |
| Crystal system | monoclinic | triclinic |
| Space group | C2/c | P-1 |
| *a*/Å | 17.5924(13) | 11.0599(10) |
| *b*/Å | 16.7807(12) | 12.4532(10) |
| *c*/Å | 20.6012(15) | 22.2391(18) |
| *α*/° | 90 | 101.704(3) |
| *β*/° | 110.266(2) | 103.402(3) |
| *γ*/° | 90 | 95.429(3) |
| Volume/Å$^3$ | 5705.2(7) | 2885.2(4) |
| Z | 4 | 2 |
| $\rho_{calc}$ g/cm$^3$ | 1.608 | 1.663 |
| $\mu$/mm$^{-1}$ | 2.704 | 2.639 |
| *F*(000) | 2704.0 | 1428.0 |
| Reflections collected | 40832 | 66850 |
| Independent reflections | 5072 [$R_{int}$ = 0.0970, $R_{sigma}$ = 0.0517] | 10259 [$R_{int}$ = 0.0557, $R_{sigma}$ = 0.0326] |
| Goodness-of-fit on $F^2$ | 1.045 | 1.035 |
| Final R indexes [I>=2σ (I)] | $R_1$ = 0.0384, $wR_2$ = 0.1021 | $R_1$ = 0.0294, $wR_2$ = 0.0821 |
| Final R indexes [all data] | $R_1$ = 0.0486, $wR_2$ = 0.1100 | $R_1$ = 0.0380, $wR_2$ = 0.0863 |

[a] $R_1 = \Sigma||F_0| - |F_c||/\Sigma|F_0|$. [b] $wR_2 = [\Sigma w(F0^2 - Fc^2)^2/\Sigma w(F0^2)^2]^{1/2}$

**Table S2. The comparison of CO evolution rate of reported MOFs for converting $CO_2$ to CO under visible light irradiation**

| Catalyst | Light source (nm) | Photosensitizer | CO production rate | Reference |
|---|---|---|---|---|
| PCN-250-$Fe_2Mn$ | 420<λ<800 | $[Ru(bpy)]Cl_2$ | 21.51 mmol $g^{-1}$ $h^{-1}$ | Appl. Catal. B: Environ. 2020, 276, 119173. |
| PCN-250-$Fe_3$ | 420<λ<800 | $[Ru(bpy)]Cl_2$ | 13.45 mmol $g^{-1}$ $h^{-1}$ | |
| BIF-101 | λ≥420 | $[Ru(bpy)]Cl_2$ | 5830 μmol $g^{-1}$ $h^{-1}$ | J. Mater. Chem. A, 2019, 7, 17272-17276 |
| **Compound 2** | **λ≥420** | **$[Ru(bpy)]Cl_2$** | **5625 μmol $g^{-1}$ $h^{-1}$** | **This work** |
| (Co/Ru)n-UiO-67(bpydc) | λ>450 | $[Ru(bpy)]Cl_2$ | 4520 μmol $g^{-1}$ $h^{-1}$ | Appl. Catal. B: Environ. 2019, 245, 496-501. |
| 2D-$Co_2$TCPE-PE | λ≥420 | $[Ru(bpy)]Cl_2$ | 4147 μmol $g^{-1}$ $h^{-1}$ | Angew. Chem., Int. Ed., 2020, 59, 23588 – 23592 |
| **Compound 1** | **λ≥420** | **$[Ru(bpy)]Cl_2$** | **3811 μmol $g^{-1}$ $h^{-1}$** | **This work** |
| BIF-29 | λ≥420 | $[Ru(bpy)]Cl_2$ | 3334 μmol $g^{-1}$ $h^{-1}$ | Angew. Chem., Int. Ed., 2019, 58, 11752-11756 |
| 2D-$Ni_2$TCPE-PE | λ≥420 | $[Ru(bpy)]Cl_2$ | 3000 μmol $g^{-1}$ $h^{-1}$ | Angew. Chem., Int. Ed., 2020, 59, 23588 – 23592 |
| 2D-$Ni_2$TCPE-ME | λ≥420 | $[Ru(bpy)]Cl_2$ | 2944 μmol $g^{-1}$ $h^{-1}$ | |
| 2D-$Co_2$TCPE | λ≥420 | $[Ru(bpy)]Cl_2$ | 2560 μmol $g^{-1}$ $h^{-1}$ | |
| 2D-$Ni_2$TCPE | λ≥420 | $[Ru(bpy)]Cl_2$ | 2000 μmol $g^{-1}$ $h^{-1}$ | |
| MOF-Co | λ≥420 | $[Ru(bpy)]Cl_2$ | 1140 μmol $g^{-1}$ $h^{-1}$ | ACS Catal. 2019, 9, 1726-1732. |
| MOF-Ni | λ≥420 | $[Ru(bpy)]Cl_2$ | 371.6 μmol $g^{-1}$ $h^{-1}$ | |
| MOF-525-Co | λ≥420 | — | 201.6 μmol $g^{-1}$ $h^{-1}$ | Angew. Chem., Int. Ed., 2016, 55, 14310-14314. |
| Co-ZIF-9 | λ>420 | $[Ru(bpy)]Cl_2$ | 83.6 μmol h-1 | Angew. Chem., Int. Ed., 2014, 53, 1034-1038. |

**Table S3. The comparison of the photocatalytic selectivity of reported MOFs for converting $CO_2$ to CO under visible light irradiation**

| Catalyst | Light source (nm) | Photosensitizer | Selectivity (%) | Reference |
|---|---|---|---|---|
| MAF-X27/-OH | λ≥420 | $[Ru(bpy)]Cl_2$ | 98.2 | J. Am. Chem. Soc. 2018, 140, 38-41. |
| MOF-Ni | λ≥420 | $[Ru(bpy)]Cl_2$ | 97.7 | ACS Catal. 2019, 9, 1726-1732. |
| 2D-$Ni_2$TCPE-PE | λ≥420 | $[Ru(bpy)]Cl_2$ | 97.31 | Angew. Chem., Int. Ed., 2020, 59, 23588 – 23592 |
| 2D-$Ni_2$TCPE | λ≥420 | $[Ru(bpy)]Cl_2$ | 97.21 | |
| 2D-$Ni_2$TCPE-ME | λ≥420 | $[Ru(bpy)]Cl_2$ | 96.93 | |
| **Compound 1** | **λ≥420** | **$[Ru(bpy)]Cl_2$** | **94.85** | **This work** |
| **Compound 2** | **λ≥420** | **$[Ru(bpy)]Cl_2$** | **94.46** | **This work** |
| BIF-101 | λ≥420 | $[Ru(bpy)]Cl_2$ | 84.1 | J. Mater. Chem. A, 2019, 7, 17272-17276 |
| BIF-29 | λ≥420 | $[Ru(bpy)]Cl_2$ | 82.6 | Angew. Chem., Int. Ed., 2019, 58, 11752-11756 |
| PCN-250-Fe2Mn | 420<λ<800 | $[Ru(bpy)]Cl_2$ | 82.2 | Appl. Catal. B: Environ. 2020, 276, 119173. |
| 2D-$Co_2$TCPE | λ≥420 | $[Ru(bpy)]Cl_2$ | 75.76 | Angew. Chem., Int. Ed., 2020, 59, 23588 – 23592 |
| PCN-250-Fe3 | 420<λ<800 | $[Ru(bpy)]Cl_2$ | 75.5 | Appl. Catal. B: Environ. 2020, 276, 119173. |
| 2D-$Co_2$TCPE-PE | λ≥420 | $[Ru(bpy)]Cl_2$ | 74.36 | Angew. Chem., Int. Ed., 2020, 59, 23588 – 23592 |
| Co-ZIF-9 | λ>420 | $[Ru(bpy)]Cl_2$ | 58 | Angew. Chem., Int. Ed., 2014, 53, 1034-1038. |
| MOF-Co | λ≥420 | $[Ru(bpy)]Cl_2$ | 47.4 | ACS Catal. 2019, 9, 1726-1732. |
| ZIF-8 | λ≥420 | $[Ru(bpy)]Cl_2$ | 47.4 | Appl. Catal. B: Environ. 2017, 209, 476-482 |
| Zr-UIO-66-$NH_2$ | λ≥420 | $[Ru(bpy)]Cl_2$ | 42.8 | |